applied sciences

MDPI

Article

Experimental Thermodynamic Investigation on the Refrigerant Charge in a Transcritical CO_2 Electric Bus Air Conditioning System

Haidan Wang [1], Shengbo Li [1], Yulong Song [1,*], Xiang Yin [1], Feng Cao [1,*] and Paride Gullo [2]

[1] School of Energy and Power Engineering, Xi'an Jiaotong University, 28 Xianning West Road, Xi'an 710049, China; haidanwang@stu.xjtu.edu.cn (H.W.); shuaibo007@stu.xjtu.edu.cn (S.L.); xiangyin@mail.xjtu.edu.cn (X.Y.)

[2] Department of Mechanical Engineering, Technical University of Denmark (DTU), Nils Koppels Allé, Building 403, 2800 Kgs. Lyngby, Denmark; parigul@mek.dtu.dk

* Correspondence: yulong.song@mail.xjtu.edu.cn (Y.S.); fcao@mail.xjtu.edu.cn (F.C.); Tel.: +86-29-82663583 (Y.S.); +86-29-82663583 (F.C.)

Abstract: Due to its considerable impact on climate, bus air conditioning systems are being pushed to take a new and sustainable path. Electric buses relying on transcritical CO_2 air conditioning units are perceived to be eco-friendly and future-proof solutions to achieving such a target. However, in order to have highly efficient air conditioning systems, the CO_2 charge needs to be optimized. In this paper the energy and exergy-based analyses were performed to investigate the effect of normalized refrigerant charge on the system performance by using a test rig of a transcritical CO_2 air conditioning unit for an 8 m electric bus. Results showed that the normalized refrigerant charge range of 0.248~0.336 was recommended in order to ensure the maximum coefficient of performance (COP). In addition, in sufficient charge conditions, the optimal COP, cooling capacity and exergy efficiency were 1.716, 18.97 kW and 29.79%, respectively, under the standard refrigeration condition of 35 °C/27 °C. As the ambient temperature rose from 35 °C to 40 °C, the COP, cooling capacity and exergy efficiency decreased by 16.03%, 10.90% and 12.22%, respectively. Furthermore, the exergy efficiency was found not to be sensitive to slightly insufficient charge, whereas overcharge was observed to be even beneficial to exergy efficiency under the condition of ensuring the maximum COP. In addition, insufficient refrigerant charging seriously affected the irreversible losses in the indoor and outdoor heat exchangers, whereas slight overcharge had little effect on the component exergy efficiency. Finally, the need to improve the CO_2 compressor efficiency to enhance the system performance was revealed.

Keywords: transcritical CO_2 system; electric bus; refrigerant charge; exergy; experimental investigation; R744

check for updates

Citation: Wang, H.; Li, S.; Song, Y.; Yin, X.; Cao, F.; Gullo, P. Experimental Thermodynamic Investigation on the Refrigerant Charge in a Transcritical CO_2 Electric Bus Air Conditioning System. *Appl. Sci.* **2021**, *11*, 5614. https://doi.org/10.3390/app11125614

Received: 10 May 2021
Accepted: 14 June 2021
Published: 17 June 2021

Publisher's Note: MDPI stays neutral with regard to jurisdictional claims in published maps and institutional affiliations.

Copyright: © 2021 by the authors. Licensee MDPI, Basel, Switzerland. This article is an open access article distributed under the terms and conditions of the Creative Commons Attribution (CC BY) license (https://creativecommons.org/licenses/by/4.0/).

1. Introduction

Electricity as an energy vector for vehicle propulsion promotes the use of renewable and carbon-free energy sources in addition to favoring energy supply security as well as lowering air pollution. Therefore, the uptake of electric vehicles [1], including buses [2], is increasing considerably worldwide. On the one hand, at present, hydrofluorocarbons (HFCs) are the most widely used refrigerants for bus air conditioning systems, especially R407C and R410A [3], which have a high value of global warming potential (GWP). On the other hand, the wide adoption of the Kigali Amendment will result in HFC cut by around 85% before 2050 on a global basis, leading low-to-zero GWP refrigerants to take center stage in transport sector. CO_2 is a widely used natural working fluid (R744) with negligible GWP, zero ozone depletion potential (ODP), low cost and excellent thermo-physical properties in addition to being non-flammable and non-toxic [4]. In addition, transcritical CO_2 systems

have considerable advantages in heating performance, especially at low-temperature heating conditions, which can solve the problem of large power consumption of electric vehicles in winter [5–8]. Therefore, transcritical CO_2 systems have great potential to become future-proof solutions for electric vehicle air conditioning units.

There are many factors that affect the coefficient of performance (COP) of the transcritical CO_2 systems [9–11], refrigerant charge being one of the most crucial ones [12]. Compared with the traditional vapor compression systems using HFCs, the performance of transcritical CO_2 systems is more sensitive to the refrigerant charge [13]. Baek et al. [14] experimentally investigated the cooling performance of a CO_2 heat pump unit by varying the refrigerant charge amount, electronic expansion valve (EEV) opening degree, compressor frequency and outdoor fan speed at various outdoor temperatures. The results showed that the optimum normalized charge is 0.712 to achieve the maximum COP at the standard cooling condition (outdoor temperature of 35 °C, indoor temperature of 27 °C) with the compressor frequency of 45 Hz and a superheating degree of 5 K. The performance of a transcritical system was experimentally evaluated under different refrigerant charge amounts by Aprea et al. [15]. The influence of the refrigerant charge on COP, cooling capacity, compression ratio and suction line superheat was analyzed in detail and the maximum COP was assessed at the optimal refrigerant charge of 7.5 kg. Hazarika et al. [12] presented a steady-state simulation model developed for a transcritical CO_2 air conditioning system. The authors found that the variation in COP is marginal for a charge variation of ±18% from the optimum value.

However, to the best of the authors' knowledge, there is only limited research on refrigerant charge of CO_2 mobile air conditioning (MAC) systems. In addition, most of the research focuses on the systems of passenger cars. Liu et al. [16] found that undercharged CO_2 systems lead to a fast decrease of the cooling capacity and COP, whereas overcharged CO_2 systems cause an abrupt increase of the compressor power input. Wang et al. [17] experimentally investigated the charge characteristics and refrigerant migration behavior of an electric transcritical CO_2 MAC unit. The authors observed that a plateau region involving the optimal system performance occurred for a refrigerant charge between 1100 g and 1600 g at 35 °C, for which COP and cooling capacity achieved their optimal performance of 1.87 and 3.5 kW, respectively. An experimental study on the normalized refrigerant charge (NRC) of the MAC system was carried out by Yin et al. [18] who found that the optimal NRC range for a transcritical CO_2 air conditioning system was between 0.111 and 0.321. Dong et al. [19] experimentally compared the COPs and cooling/heating capabilities of MAC systems using R134a and CO_2 as work fluid. The optimal CO_2 charge amount was determined to be 600~650 g and the COP can reach 1.36 and 2.16 at 40 °C (cooling mode) and −20 °C (heating mode), respectively. Different from the above studies, Song et al. [20,21] experimentally investigated the cooling and heating performance of a transcritical CO_2 MAC system for an electric bus. The results showed an optimal COP of 2.88 and a cooling capacity of 31.4 kW at 9 kg charge amount in cooling mode (outdoor temperature of 35 °C and indoor temperature of 19.5 °C) as well as an optimal COP of 1.78 and a heating capacity of 15.3 kW at 8.8 kg in heating mode (outdoor temperature of −20 °C and indoor temperature of 20 °C). From the literature above it can be concluded that there is little research on transcritical CO_2 air conditioning systems for electric buses. In order to fill this research gap, a test rig of an electric bus air conditioning system was built and employed for evaluating the influence of the refrigerant charge on the performance of the air conditioning unit based on the energy and exergy analyses.

2. Materials and Methods

2.1. Experimental Setup Description

The schematic of the employed test rig, i.e., a transcritical CO_2 air conditioning system for an 8 m electric bus, is shown in Figure 1. It consists of an electrical compressor, two indoor heat exchangers (HXs), an outdoor HX, an EEV and an accumulator. The compressor used in the test rig is a rotary type with double cylinders and whose displacement is

5.4 $m^3 \cdot h^{-1}$ at 3600 RPM. In addition, its speed can vary from 1800 RPM to 5400 RPM. The high pressure and the compressor discharge temperature could not be above 12 MPa and 120 °C, respectively, due to safety reasons. The indoor HXs and the outdoor HX are fin tube heat exchangers. Four axial flow fans were installed on the outdoor HX, while two centrifugal fans were mounted on each indoor HX. The 4.8 L accumulator is located upstream of the compressor suction pipe to protect the compressor and enhance the system adaptability under different working conditions. A Saginomiya JKV-24D EEV was used in the system, and it was driven by a stepper motor, whose operating range is 0–480 step. The specifications of each component are listed in Table 1.

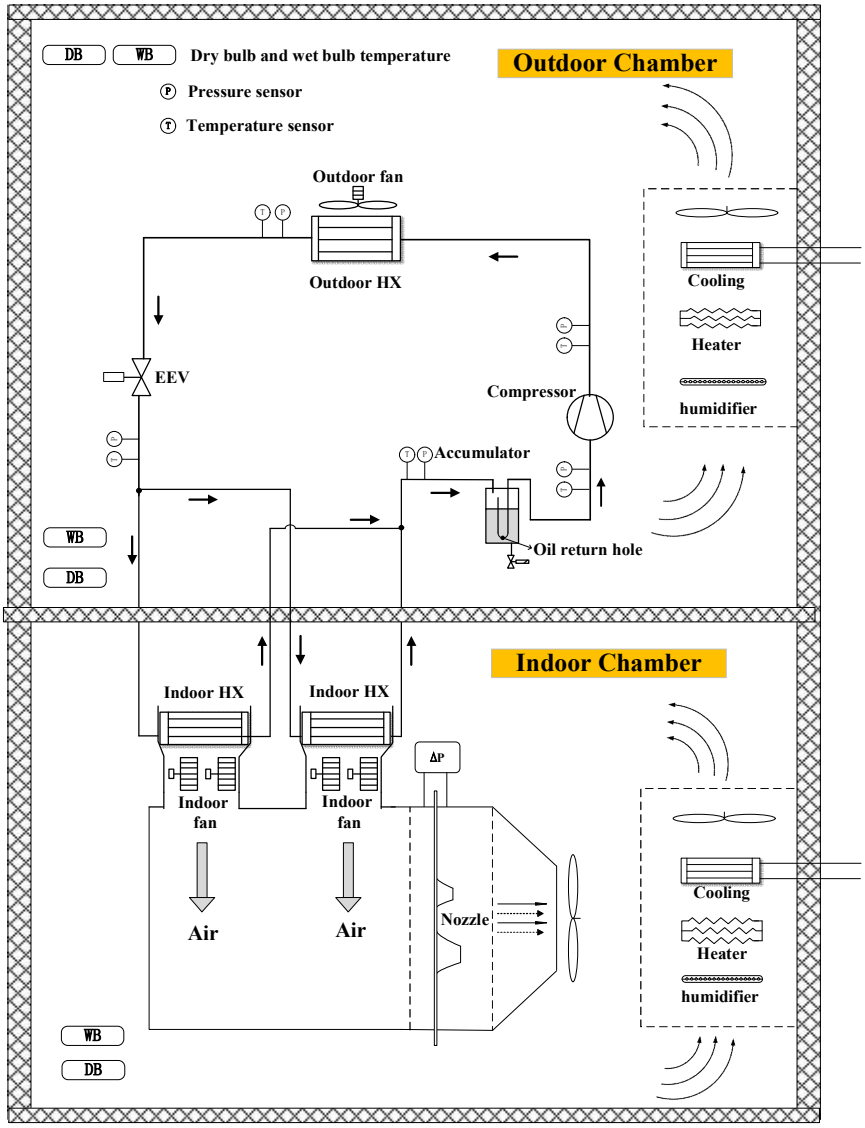

Figure 1. Schematic diagram of the transcritical CO_2 electric bus air conditioning system test rig.

Table 1. Specifications on system components.

Equipment Name	Quantity	Specification
Compressor	1	Type: Rotary compressor Displacement: 5.4 m^3 h^{-1} at 3600 RPM Speed range: 1800~5400 RPM
Outdoor HX	1	Type: Fin tube heat exchanger Dimension: 1530 mm (length), 76.2 mm (width), 210 mm (height) Tube (mm): Φ7 × 0.7 copper tube Fin material: Aluminum Fins per inch: 15.875 Fin thickness (mm): 0.2
Indoor HX	2	Type: Fin tube heat exchanger Dimension: 1150 mm (length), 76.2 mm (width), 162 mm (height) Tube (mm): Φ7 × 0.7 copper tube Fin material: Aluminum Fins per inch: 15.875 Fin thickness (mm): 0.2
EEV	1	Range of 0–480 step Driven by a stepper motor
Accumulator	1	4.8 L

2.2. Test Procedures

To investigate the impacts of refrigerant charge on system performance in the transcritical CO_2 refrigeration system for electric buses, a series of steady-state tests were conducted under different refrigerant charges, different EEV opening degrees and different ambient temperatures. The experiments were carried out in the upper and lower separated enthalpy difference chamber, both of which can independently control the environment temperature and humidity. The photos of the test rig in both parts of the enthalpy difference chamber are shown in Figure 2. The outdoor ambient temperatures were set to 35 °C, 38 °C and 40 °C in the experiments, while the indoor dry/wet bulb temperatures were set to 27 °C/19.5 °C. Furthermore, the air flow rates of the indoor and outdoor fans were kept constant at 3100 $m^3 \cdot h^{-1}$ and 8800 $m^3 \cdot h^{-1}$, respectively. The discharge pressure and temperature of the compressor were controlled to not exceed the aforementioned safety limits, while the compressor speed was set to 3600 RPM in the whole experimental campaign. In addition, the opening of the EEV is reduced by 30 steps per second in the beginning and 10 steps when the system is close to the optimal state. The optimal values of each parameter were obtained in the experiment.

Furthermore, Beak et al. [14] proposed the concept of a normalized refrigerant charge (NRC) to eliminate the effect of the system volume. The actual charge in the various unit scales can be normalized as indicated in Equation (1). The NRC varies from 0 to 1.

$$\mathrm{NRC} = \frac{M_{actual} - M_{vapor}}{M_{liquid} - M_{vapor}} \quad (1)$$

in which M_{actua1} is the actual refrigerant charge (kg) while M_{vapor} and M_{liquid} are the corresponding refrigerant charges (kg) at saturation conditions. The values of M_{vapor} and M_{liquid} can be obtained by multiplying the system internal volume with the refrigerant densities at the saturation conditions evaluated at the ambient temperature of 25 °C. Table 2 shows the normalized charge value.

Figure 2. Photos of the transcritical CO_2 electric bus air conditioning system rig.

Table 2. The actual charge and corresponding normalized charge.

M_{actual} (kg)	Normalized Charge
3.750	0.034
4.200	0.100
4.450	0.137
4.900	0.204
5.200	0.248
5.500	0.292
5.800	0.336
6.100	0.381

2.3. Data Processing

2.3.1. Energy Analysis

The cooling capacity of the CO_2 transcritical system for the electric bus was evaluated from the air side given in Equation (2) as follows:

$$\dot{Q}_{cooling} = \frac{\dot{V}_a * \rho_a * (h_{a,in} - h_{a,out})}{3600} \quad (2)$$

in which $\dot{V}_a$ is the volume flow rate of the air ($m^3 \cdot h^{-1}$), ρ_a is the density of the air ($kg \cdot m^{-3}$), $h_{a,in}$ and $h_{a,out}$ are the enthalpy of the air at the inlet and outlet of the electric bus cabin ($kJ \cdot kg^{-1}$), respectively; and 3600 represents the conversion of hours to seconds.

The enthalpies of the air $h_{a,in}$ and $h_{a,out}$ were evaluated as a function of the measured dry-bulb temperature and wet-bulb temperature as follows:

$$h_a = f\left(T_{a,dry-bulb}, T_{a,wet-bulb}\right) \quad (3)$$

The COP was calculated by Equation (4), in which the $\dot{W}_{tot}$ refers to the power input of compressor and fans as follows:

$$\mathrm{COP} = \frac{\dot{Q}_{cooling}}{\dot{W}_{tot}} \quad (4)$$

Since there is no internal heat exchanger in the system, the CO_2 fluid suctioned by the compressor could be in the vapor-liquid state when the charge amount is large. At this time, the enthalpy of the CO_2 at inlet of the compressor is calculated by Equation (5):

$$h_{com,suc} = \frac{h_{e,in} + \mathrm{COP} * h_{com,out}}{1 + \mathrm{COP}} \quad (5)$$

in which $h_{com,suc}$ and $h_{com,out}$ are the enthalpy of the CO_2 at inlet and outlet of the compressor, respectively, and $h_{e,in}$ is the enthalpy of the CO_2 at inlet of the evaporator.

2.3.2. Exergy Analysis

The exergy of a system is the maximum valuable work possible during a process, bringing the system into equilibrium with a heat reservoir. The system boundary, as shown in the Figure 3 was used in the calculation of exergy efficiency. In conformity with the work by Gullo et al. [22,23], the conventional exergy analysis was performed by applying Equation (6) to each component of the investigated system. Equation (6) represents the exergy rate balance within the selected control volume (i.e., the selected component) at steady state conditions, allowing for the assessment of the source of its thermodynamic inefficiencies by calculating its exergy destruction rate ($\dot{E}_D$). Equation (6) is presented as follows:

$$\sum_j \left(1 - \frac{T_0}{T_j}\right) \cdot \dot{Q}_j - \dot{W} + \sum_{in} \dot{m}_{in} \cdot e_{in} - \sum_{out} \dot{m}_{out} \cdot e_{out} - \dot{E}_D = 0 \quad (6)$$

in which the term $\left(1 - T_0/T_j\right) \cdot \dot{Q}_j$ indicates the exergy transfer rate related to heat transfer at the rate $\dot{Q}_j$ occurring at the location on the boundary characterized by a temperature T_j, while the term $\dot{W}$ accounts for power. The specific exergy of the selected component was calculated as follows:

$$\mathrm{e} = h - h_0 - T_0(s - s_0) \quad (7)$$

in which h_0 (kJ·kg^{-1}) and s_0 (kJ·(kg^{-1}·K^{-1})) are the enthalpy and entropy of working medium calculated at the dead state, i.e., T_0 = 308.15 K, 311.15 K and 313.15 K (ambient temperature of system operation) and p_0 = 0.1013 MPa. It is important to highlight that the kinetic, chemical and potential exergy variations are negligible for all vapor compression systems.

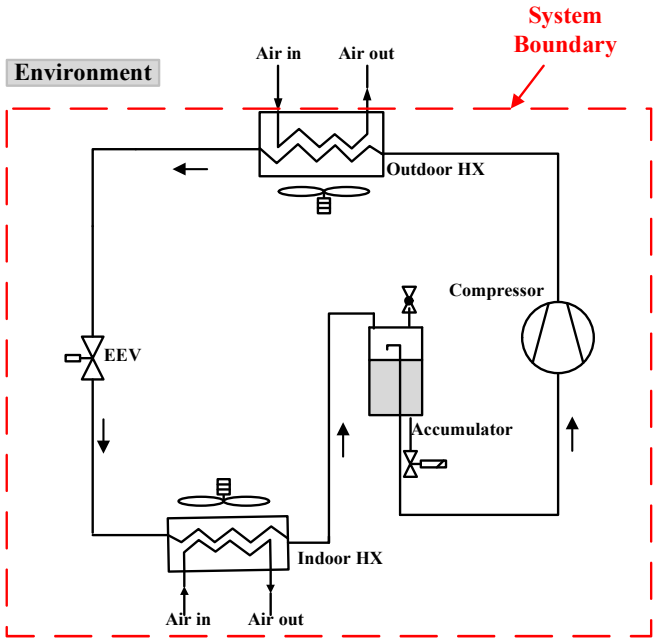

Figure 3. The boundary in the exergy analysis.

The specific exergy of air can be calculated by Equation (8) [24] as follows:

$$\begin{aligned} e_a &= (c_{P,a} + \omega_a c_{P,v})(T_a - T_0) \\ &\quad -T_0\left[(c_{P,a} + \omega_a c_{P,v})ln\left(\frac{T_a}{T_0}\right) - (R_a + \omega_a R_v)ln\left(\frac{P_a}{P_0}\right)\right] \\ &\quad +T_0\left[(R_a + \omega_a R_v)ln\left(\frac{1+1.6078\omega_0}{1+1.6078\omega_a}\right)\right. \\ &\quad \left.+1.6078\omega_a R_a ln\left(\frac{\omega_a}{P\omega_0}\right)\right] \end{aligned} \tag{8}$$

for which ω_a is the absolute humidity of air ($kg_{water}/kg_{dry\ air}$); R_a and R_v are the air and vapor constant (kJ·(kg^{-1}·K^{-1}); and $c_{P,a}$ and $c_{P,v}$ are the specific heat of air and vapor at constant pressure (kJ·(kg^{-1}·°C^{-1}).

The total product exergy rate of the investigated air conditioning unit ($\dot{E}_P$) was:

$$\dot{E}_{P,tot} = \dot{W}_{tot} - \dot{E}_{D,tot} - \dot{E}_{loss,tot} \tag{9}$$

in which the exergy loss rate $\dot{E}_{loss,tot}$ (kW) refers to the exergy rate of the air flowing through the gas cooler. In this paper, $\dot{E}_{loss,tot}$ was neglected.

The exergy efficiency (η) of the transcritical CO_2 cycle was calculated as

$$\eta = 1 - \frac{\dot{E}_{D,tot}}{\dot{W}_{tot}} \tag{10}$$

2.4. Uncertainty Analysis

The detailed information of the measuring instruments is listed in Table 3.

Table 3. Detailed information of the measuring instruments.

Parameter	Instrument	Accuracy	Range
Refrigerant temperature	T-type	±0.20 °C	−50–200 °C
Air dry/wet bulb temperature	Pt100	±0.20 °C	−200–450 °C
Refrigerant pressure	Pressure transmitters	±0.25% of full range	0–15 MPa
Air volume flow rate	Standard nozzle device	±0.50% of reading	0~10,000 m^3·h^{-1}
Power input	Electric power analyzer	±0.16% of reading	9~600 V
Charge amount	Electronic mass scale	±20.00 g	0.020~40.000 A

The uncertainty propagation analysis was performed by using the Kline and McClintock method [25], expressed in the following equation:

$$\omega_R = \left[\left(\frac{\partial R}{\partial x_1}\omega_1\right)^2 + \left(\frac{\partial R}{\partial x_2}\omega_2\right)^2 + \cdots + \left(\frac{\partial R}{\partial x_n}\omega_n\right)^2\right]^{1/2} \tag{11}$$

where ω_R is the resulting uncertainty, $\omega_1, \omega_2, \ldots, \omega_n$ are the uncertainties of the independent variables $x_1, x_2, \ldots, x_n$. According to this method, the maximum uncertainties of $\dot{Q}_{cooling}$, COP and η were estimated to be ±6.51%, ±6.68% and ±5.84%, respectively. The thermo-physical properties of CO_2 and air were derived from *NIST REFPROP* [26] during the data reduction process.

3. Results and Discussion

3.1. Energy Analysis

Figure 4 presents the variation of the COP_{opt}, cooling capacity ($\dot{Q}_{cooling}$), optimal discharge pressure ($P_{dis,opt}$), outlet pressure of the evaporator ($P_{e,out}$) and the optimal EEV opening degree (OD_{opt}) with respect to NRC. The values of OD_{opt} as a function of NRC were kept the same at all the selected ambient temperatures, since they were not affected by the latter considerably. The states of sufficient charge showed in Figure 4 (i.e., NRC

values between 0.248 and 0.336) refer to the operating conditions at which the COP values are maximized. On the other hand, the excessive and insufficient states in Figure 4 indicate the operating conditions above and below those involving COP_{max} values, respectively. The OD_{opt} reached the minimum value of 0.479 at sufficient charge states, and at the same time, the optimal discharge pressures were 10.9 MPa, 11.5 MPa and 11.63 MPa at 35 °C, 38 °C and 40 °C, respectively. The highest values of COP_{opt} and $\dot{Q}_{cooling}$ were about 1.716 and 18.97 kW at 35 °C, 1.543 and 17.69 kW at 38 °C and 1.441 and 16.90 kW at 40 °C. As the ambient temperature rose from 35 °C to 40 °C, the COP and cooling capacity of the system decreased by 16.03% and 10.90%, respectively. For low values of NRC, the system performance was found to be very poor. As the NRC was 0.204, the COP and $\dot{Q}_{cooling}$ decreased by 1.39% and 4.06% at 35 °C, by 3.56% and 5.94% at 38 °C and by 7.04% and 9.44% at 40 °C compared to corresponding cases involving NRC values between 0.248 and 0.336, respectively. As the NRC was 0.380, the COP and $\dot{Q}_{cooling}$ decreased by 2.59% and 3.22% at 35 °C, by 1.25% and 0.50% at 38 °C and by 2.91% and 1.51% at 40 °C compared to the corresponding cases involving NRC values between 0.248 and 0.336. It could be concluded that the effect of insufficient charge on cooling capacity is more penalizing than that of a slight overcharge.

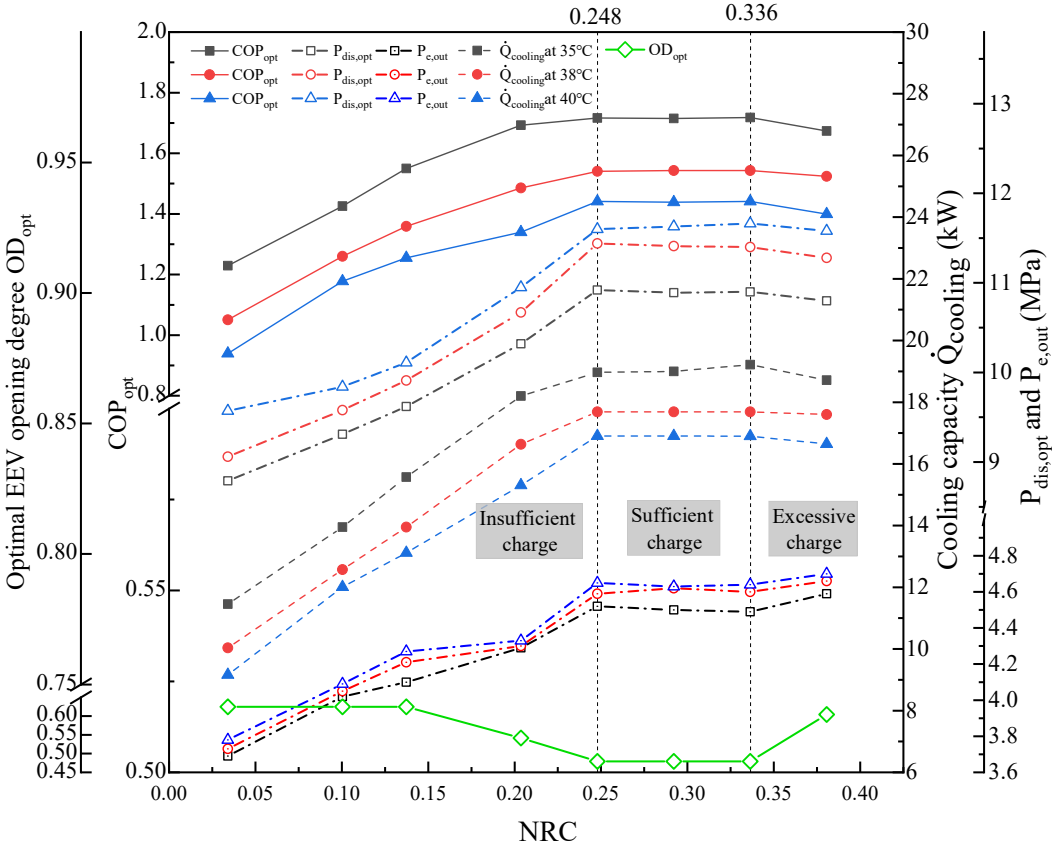

Figure 4. The effect of normalized refrigerant charge (NRC) on COP_{opt}, cooling capacity ($\dot{Q}_{cooling}$), optimal discharge pressure ($P_{dis,opt}$), outlet pressure of evaporator ($P_{e,out}$) and optimal EEV opening degree (OD_{opt}) at ambient temperatures of 35 °C, 38 °C and 40 °C.

Figure 5a shows the variation of COP and $\dot{Q}_{cooling}$ with discharge pressure when the NRC is 0.137 (insufficient charge condition), 0.248 (sufficient charge condition) and 0.381 (excessive charge condition) at 35 °C. It was found that as P_{dis} reached the optimal value, both COP and $\dot{Q}_{cooling}$ reached the maximum values. Furthermore, when the discharge pressure was higher than $P_{dis,opt}$, both COP and $\dot{Q}_{cooling}$ decreased significantly in the insufficient charge condition, whereas they declined more slightly in the sufficient charge

condition. However, in the excessive charge condition, as the COP started decreasing slightly, $\dot{Q}_{cooling}$ was still increasing significantly. These phenomena were caused by the migration characteristics of the refrigerant. Figure 5b depicts the P-h diagrams of the investigated system at the aforementioned three conditions at different EEV opening degrees. As the value of OD decreased from 1 to 0.417, P_{dis} increased slightly (from 9.25 MPa to 9.78 MPa) and P_{suc} reduced from 4.58 MPa to 3.63 MPa under the insufficient charge condition. The variation of P_{suc} was more marked than P_{dis} with the rise in OD, leading to a significant increase in the superheating degree of the system and thus to a sharp reduction of the CO_2 mass flow rate. Although the enthalpy difference in indoor HXs increased, the cooling capacity was found to reduce. With the rise in refrigerant charge, the amount of refrigerant in the indoor HXs and outdoor HX increased. Additionally, the P_{suc} decreased slightly and the P_{dis} increased with the reduction in OD. Under the sufficient charge condition, P_{dis} increased from 10.04 MPa to 11.17 MPa and the P_{suc} reduced from 5.02 MPa to 4.53 MPa as the value of OD decreased from 1 to 0.417. In addition, as OD was lower than the optimal value, the refrigerant drawn by the compressor was superheated vapor and its superheating degree increased with decrease in EEV opening degree, resulting in a slight reduction in cooling capacity. Under the excessive charge condition, P_{dis} sharply increased from 10.16 MPa to 11.81 MPa and the refrigerant drawn by the compressor was in the condition of a vapor–liquid mixture. Thus, the increase of enthalpy difference in the evaporators rather than the decrease of flow rate was the main factor affecting the system cooling capacity, causing an increase in cooling capacity. Therefore, it could be concluded that from the insufficient charge condition to the sufficient charge condition, the refrigerant mainly migrated to the three heat exchangers, whereas in the excessive charge condition the accumulation of refrigerant in the gas cooler was more marked than that in the evaporators.

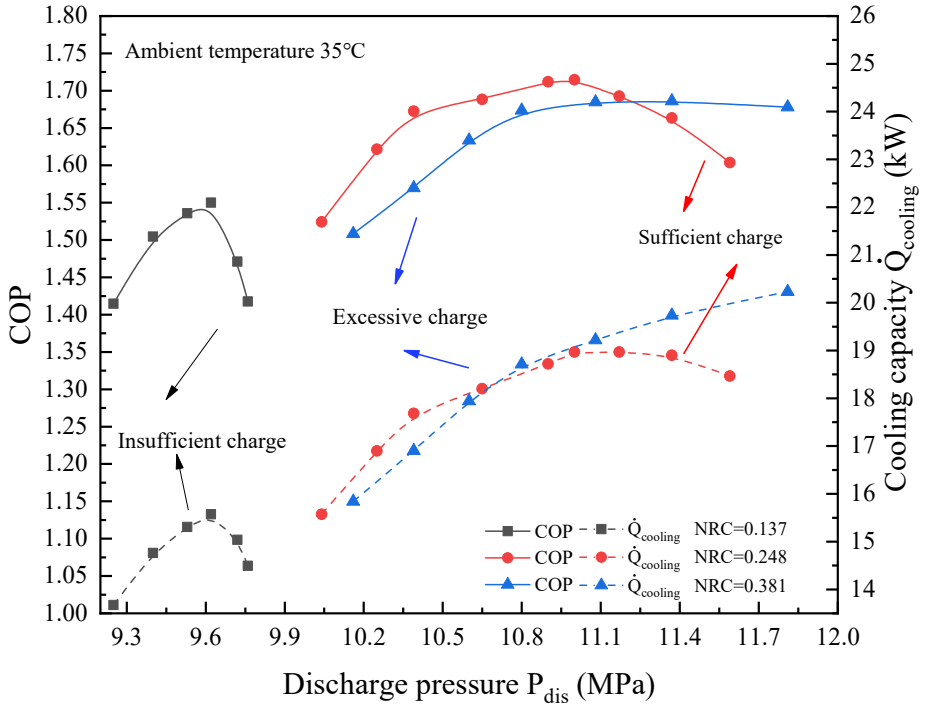

(**a**)

Figure 5. *Cont.*

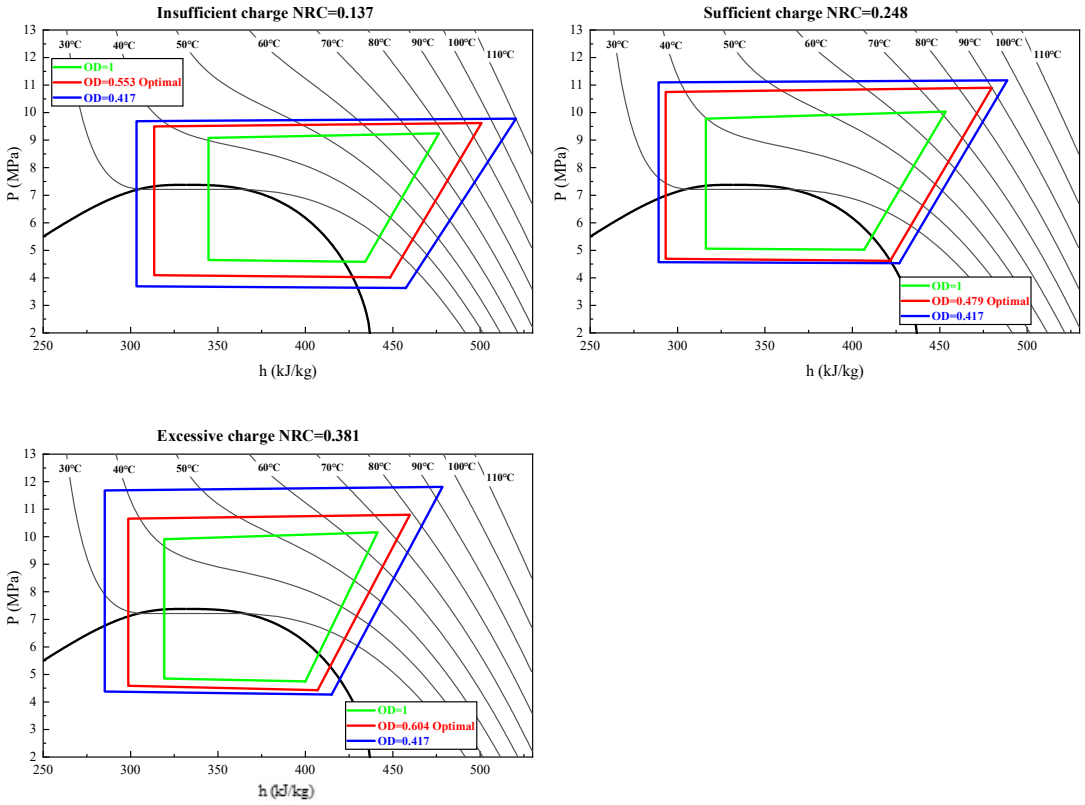

(**b**)

Figure 5. (**a**) Variation of COP and cooling capacity with discharge pressure and (**b**) P-h diagrams of the transcritical CO_2 system at the insufficient charge, sufficient charge and excessive charge at different EEV opening degrees (OD).

3.2. Exergy Analysis

Figure 6 indicates that the exergy efficiency (η) corresponding to the optimal COP increased with rise in NRC. In addition, at sufficient charge conditions, η was equal to 29.79%, 28.32% and 26.15% at 35 °C, 38 °C and 40 °C, respectively. As the ambient temperature rose from 35 °C to 40 °C, η decreased by 12.22%. It is worth noting that although the system was undercharged (i.e., NRC between 0.100 and 0.248), the exergy efficiency almost remained the same. In contrast, the value went up sharply in excessive charge conditions. However, although the compressor power input was small as the NRC was 0.10, the power input of the indoor/outdoor fans was relatively high, which led to the reduction of η. Furthermore, in the excessive charge condition, the total product exergy rate and compressor power consumption increased with the rapid rise of the CO_2 mass flow rate. Therefore, the exergy efficiency increased, since the fan power input accounted for a small proportion of the total power input. It could be concluded that the value of the η was not sensitive to slight insufficient charge, whereas overcharging the system resulted in even greater exergy efficiency under the condition of ensuring the maximum COP.

Figure 7 shows the effect of the discharge pressure (P_{dis}) on the exergy efficiency (η), the total product exergy rate ($\dot{E}_{P,tot}$), the total power input ($\dot{W}_{tot}$) and the total exergy destruction rate ($\dot{E}_{D,tot}$) at 35 °C. It can be seen from Figure 7a that the value of η first increased and then decreased with rise in P_{dis} under different charging conditions. Total power input went up almost linearly with the increase in P_{dis}, whereas the growth rate of $\dot{E}_{D,tot}$ continues to rise (shown in Figure 7b), resulting in a peak value of η. However, the P_{dis} corresponding to the maximum η of each charging condition was smaller than that of the maximum COP. The maximum value of η increased first and then decreased with the NRC increase and achieved the maximum value of 30.74% in the sufficient charging condition. In addition, similar to cooling capacity, the total product exergy rate ($\dot{E}_{P,tot}$) first

increased and then decreased with the rise in P_{dis} in the insufficient and sufficient charge conditions, whereas no peak value in the excessive charge condition was observed.

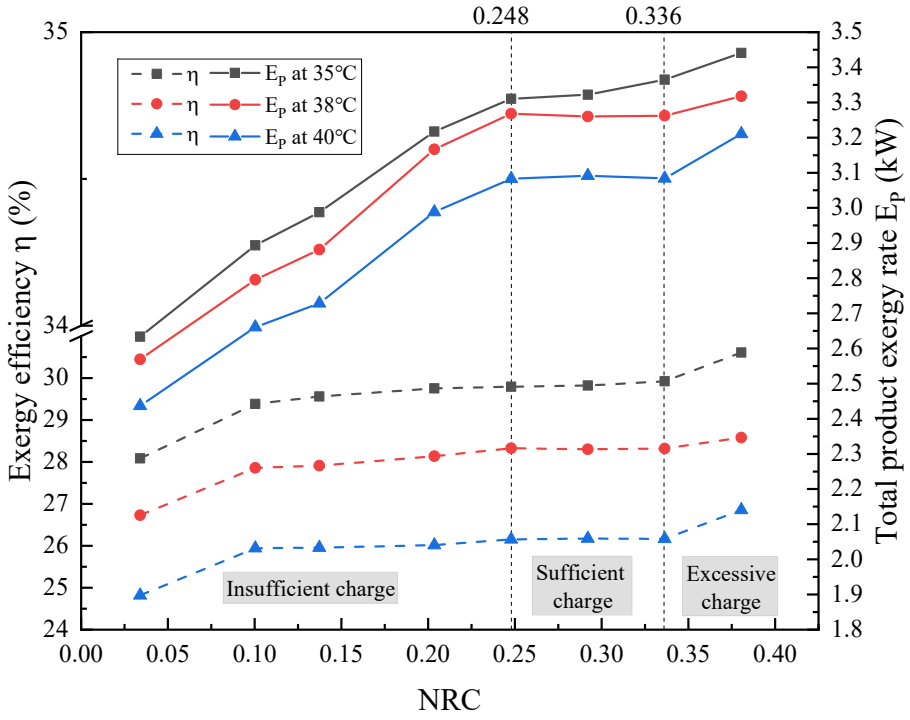

Figure 6. The effect of normalized refrigerant charge (NRC) on exergy efficiency (η) and total product exergy rate ($\dot{E}_{P,tot}$) corresponding to the optimal COP at ambient temperatures of 35 °C, 38 °C and 40 °C.

Figure 7b shows that $\dot{E}_{D,tot}$ increased significantly in insufficient charge conditions and it rose even more sharply as P_{dis} was greater than 10.9 MPa ($P_{dis,opt}$) in sufficient charge conditions. The main reason is that the temperature difference between air and refrigerant in the evaporator increased due to the low evaporator pressure. Furthermore, the refrigerant drawn by the compressor was at the state of superheated vapor under these conditions, causing an increase of T_{dis} and thus higher exergy destruction within the gas cooler.

The variation of exergy destruction percentages of the compressor, gas cooler, EEV and evaporator with NRC corresponding to the optimal COP at ambient temperature of 35 °C is shown in Figure 8. It was found that the exergy destruction percentage of the compressor varies more significantly, increasing from 24.69% to 44.27% as NRC increase from 0.100 to 0.373. This is related to the slight increase of the compressor isentropic efficiency. On the contrary, the exergy destruction percentage of the evaporator decreased from 19.78% to 7.97% mainly due to the rise of the evaporation pressure and the reduction of the heat transfer temperature difference between air and refrigerant. In the gas cooler the exergy destruction decreased gradually due to the reduction of the compressor discharge temperature. Furthermore, the CO_2 entropy difference between the inlet and outlet of the EEV decreased gradually with rise in NRC, thus the exergy destruction percentage also showed a slight downward trend. The exergy destruction percentage of the gas cooler and EEV corresponded to 22.06~27.08% and 24.13~29.63%, respectively. It could be concluded that insufficient refrigerant charging in the investigated air conditioner unit seriously affected the thermodynamic performance of the indoor and outdoor HXs, whereas slight overcharge was found to have little effect on the thermodynamic performance of each component. Finally, the obtained results suggested the need to improve the efficiency of the CO_2 compressor.

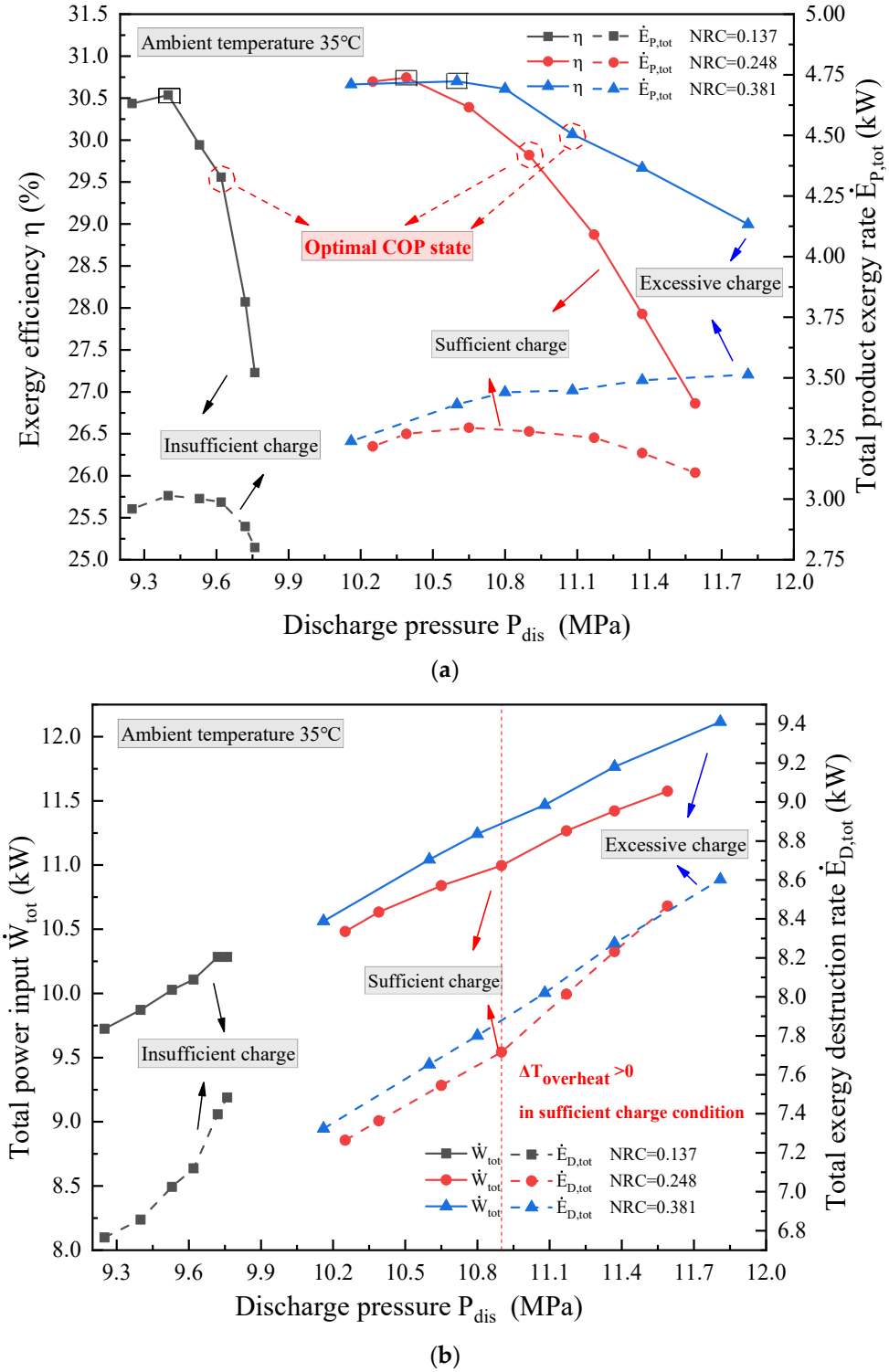

Figure 7. The effect of discharge pressure (P_{dis}) on (**a**) exergy efficiency (η) and total product exergy rate ($\dot{E}_{P,tot}$) as well as on (**b**) total power input ($\dot{W}_{tot}$) and total exergy destruction rate ($\dot{E}_{D,tot}$) at ambient temperature of 35 °C.

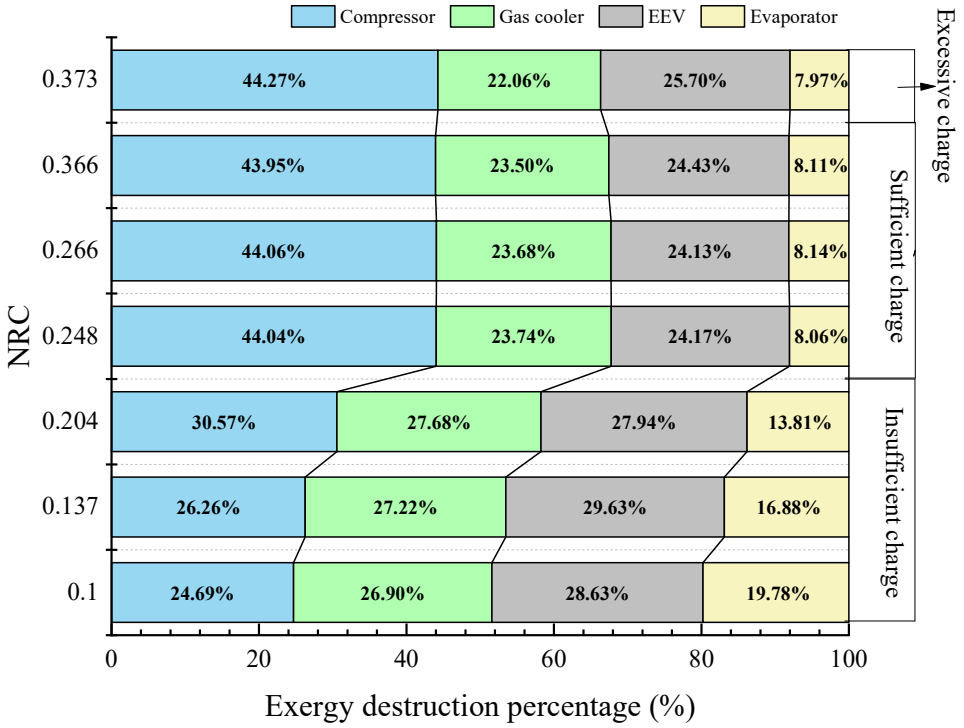

Figure 8. Variation of exergy destruction percentage of each component corresponding to the optimal COP with NRC at ambient temperature of 35 °C.

4. Conclusions

In this paper, the performance of a transcritical CO_2 air conditioning system for an electric bus has been investigated from an energy and exergy point of view. The effects of the normalized refrigerant charge, ambient temperature and EEV opening degree on the cycle performance have been analyzed in detail. The crucial conclusions are summarized below:

1. In order to ensure the maximum COP, the optimal range of the NRC is between 0.248 and 0.336 for transcritical CO_2 electric bus air conditioning units.
2. The effect of an insufficient charge on cooling capacity degradation is more penalizing than that of a slight refrigerant overcharge. This result is more evident with rise in ambient temperature.
3. The maximum value of the exergy efficiency is equal to 30.74% in the sufficient charging condition. However, the maximum value of the exergy efficiency and the optimal value of COP do not coincide.
4. Similarly to the optimal COP conditions, the exergy efficiency is not sensitive to slight insufficient charge and refrigerant overcharge is even beneficial to the exergy efficiency. In addition, insufficient refrigerant charge affected the irreversibilities in the indoor and outdoor HXs significantly, whereas slight refrigerant overcharge has little effect on the thermodynamic performance of each component. Finally, the work has revealed the need to enhance the efficiency of the compressor.

Author Contributions: Conceptualization, H.W. and Y.S.; methodology, H.W. and S.L.; software, H.W.; validation, Y.S. and S.L.; formal analysis, Y.S. and X.Y.; investigation, H.W. and S.L.; resources, Y.S. and F.C.; data curation, H.W.; writing—original draft preparation, H.W. and P.G.; writing—review and editing, All authors; visualization, H.W.; supervision, Y.S., X.Y. and F.C.; project administration, Y.S. and F.C.; funding acquisition, F.C. and Y.S. All authors have read and agreed to the published version of the manuscript.

Funding: H.W., S.L., Y.S., X.Y. and F.C. gratefully acknowledge the financial supports from the National Natural Science Foundation of China (No. 51976153 and No. 52006161).

Conflicts of Interest: The authors declare no conflict of interest.

Nomenclature

COP	Coefficient of performance
c_p	Specific heat at constant pressure, (kJ·(kg^{-1}·°C^{-1}))
EEV	Electronic expansion valve
$\dot{E}_D$	Exergy destruction rate, (kW)
$\dot{E}_{loss}$	Exergy loss rate, (kW)
$\dot{E}_P$	Product exergy rate, (kW)
e	Specific exergy, (kJ·kg^{-1})
GWP	Global warming potential
HFC	Hydrofluorocarbons
HX	Heat exchanger
h	Specific enthalpy, (kJ·kg^{-1})
$\dot{m}$	Mass flow rate, (kg·s^{-1})
M_{actual}	Actual refrigerant charge, (kg)
M_{vapor}	Mass at saturated vapor, (kg)
M_{liquid}	Mass at saturated liquid, (kg)
MAC	Mobile air conditioning
NRC	Normalized refrigerant charge
OD	EEV opening degree, (%)
ODP	Ozone depletion potential
P	Pressure, (MPa)
$\dot{Q}$	Heat transfer rate, (kW)
R	Gas constant, (kJ·kg^{-1}·K^{-1})
T	Temperature, (°C)
RPM	Round per minute, (r·min^{-1})
s	Specific entropy, (kJ·(kg^{-1}·K^{-1}))
$\dot{V}$	Air volume flow rate, (m^3·h^{-1})
$\dot{W}$	Power input, (kW)
η	Exergy efficiency, (%)
ω	Absolute humidity of air, ($kg_{water}/kg_{dry\ air}$)
ρ_{air}	Air density, (kg·m^{-3})
Subscripts	
0	Dead state
a	Air
com	Comporsor
dis	Discharge of compressor
e	Evaporater
in	Inlet
opt	Optimal
out	Outlet
r	Refrigerant
suc	Suction of compressor
tot	Total
v	Vapor

References

1. Han, X.; Zou, H.; Wu, J.; Tian, C.; Tang, M.; Guangyan, H. Investigation on the heating performance of the heat pump with waste heat recovery for the electric bus. *Renew. Energy* **2020**, *152*, 835–848. [CrossRef]
2. Kunith, A.; Goehlich, D.; Mendelevitch, R. Planning and optimization of a fast-charging infrastructure for electric urban bus systems. In Proceedings of the Second International Conference on Traffic and Transport Engineering (ICTTE), Belgrade, Serbia, 27–28 November 2014.
3. Han, X.; Zou HXu, H.; Tian, C.; Kang, W. Experimental study on vapor injection air source heat pump with internal heat exchanger for electric bus. *Energy Procedia* **2019**, *158*, 4147–4153. [CrossRef]

4. Lorentzen, G.; Pettersen, J. A new efficient and environmentally benign system for car air-conditioning. *Int. J. Refrig.* **1993**, *16*, 4–12. [CrossRef]
5. Wang, D.; Yu, B.; Li, W.; Shi, J.; Chen, J. Heating performance evaluation of a CO_2 heat pump system for an electrical vehicle at cold ambient temperatures. *Appl. Therm. Eng.* **2018**, *142*, 656–664. [CrossRef]
6. Chen, Y.; Zou, H.; Dong, J.; Wu, J.; Xu, H.; Tian, C. Experimental investigation on the heating performance of a CO_2 heat pump system with intermediate cooling for electric vehicles. *Appl. Therm. Eng.* **2021**, *182*, 116039. [CrossRef]
7. Kim, S.C.; Min, S.K.; Hwang, I.C.; Lim, T.W. Heating performance enhancement of a CO_2 heat pump system recovering stack exhaust thermal energy in fuel cell vehicles. *Int. J. Refrig.* **2007**, *30*, 1215–1226. [CrossRef]
8. Dong, J.; Wang, Y.; Jia, S.; Zhang, X.; Huang, L. Experimental study of R744 heat pump system for electric vehicle application. *Appl. Therm. Eng.* **2021**, *183*, 116191.
9. Dai, B.; Liu, S.; Sun, Z.; Ma, Y. Thermodynamic performance analysis of CO_2 transcritical refrigeration cycle assisted with mechanical subcooling. *Energy Procedia* **2017**, *105*, 2033–2038. [CrossRef]
10. Gullo, P.; Hafner, A.; Banasiak, K. Transcritical R744 refrigeration systems for supermarket applications: Current status and future perspectives. *Int. J. Refrig.* **2018**, *93*, 269–310. [CrossRef]
11. Song, Y.; Ma, Y.; Wang, H.; Yin, X.; Cao, F. Review on the simulation models of the two-phase-ejector used in the transcritical carbon dioxide systems. *Int. J. Refrig.* **2020**, *119*, 434–447. [CrossRef]
12. Hazarika, M.M.; Ramgopal, M.; Bhattacharyya, S. Studies on a transcritical R744 based summer air-conditioning unit: Impact of refrigerant charge on system performance. *Int. J. Refrig.* **2018**, *89*, 22–39. [CrossRef]
13. Cho, H.; Ryu, C.; Kim, Y.; Kin, H.Y. Effects of refrigerant charge amount on the performance of a transcritical CO_2 heat pump. *Int. J. Refrig.* **2005**, *28*, 1266–1273. [CrossRef]
14. Baek, C.; Heo, J.; Jung, J.; Cho, H.; Kim, Y. Optimal control of the gas-cooler pressure of a CO_2 heat pump using EEV opening and outdoor fan speed in the cooling mode. *Int. J. Refrig.* **2013**, *36*, 1276–1284. [CrossRef]
15. Aprea, C.; Greco, A.; Maiorino, A. An experimental study on charge optimization of a trans-critical CO_2 cycle. *Int. J. Environ. Sci. Technol.* **2015**, *12*, 1097–1106. [CrossRef]
16. Liu, H.; Chen, J.; Chen, Z. Experimental investigation of a CO_2 automotive air conditioner. *Int. J. Refrig.* **2005**, *28*, 1293–1301. [CrossRef]
17. Wang, D.; Zhang, Z.; Yu, B.; Wang, X.; Shi, J.; Chen, J. Experimental research on charge determination and accumulator behavior in transcritical CO_2 mobile air-conditioning system. *Energy* **2019**, *183*, 106–115. [CrossRef]
18. Yin, X.; Wang, A.; Fang, J.; Cao, F.; Wang, X. Coupled effect of operation conditions and refrigerant charge on the performance of a transcritical CO_2 automotive air conditioning system. *Int. J. Refrig.* **2021**, *123*, 72–80. [CrossRef]
19. Wang, Y.; Dong, J.; Jia, S.; Huang, L. Experimental comparison of R744 and R134a heat pump systems for electric vehicle application. *Int. J. Refrig.* **2021**, *121*, 10–20. [CrossRef]
20. Song, X.; Lu, D.; Lei, Q.; Wang, D.; Yu, B.; Shi, J.; Chen, J. Energy and exergy analyses of a transcritical CO_2 air conditioning system for an electric bus. *Appl. Therm. Eng.* **2021**, *190*, 116819. [CrossRef]
21. Song, X.; Lu, D.; Lei, Q.; Cai, Y.; Wang, D.; Shi, J.; Chen, J. Experimental study on heating performance of a CO_2 heat pump system for an electric bus. *Appl. Therm. Eng.* **2021**, *190*, 116789. [CrossRef]
22. Gullo, P. Advanced thermodynamic analysis of a transcritical R744 booster refrigerating unit with dedicated mechanical subcooling. *Energies* **2018**, *11*, 3058. [CrossRef]
23. Gullo, P. Impact and quantification of various individual thermodynamic improvements for transcritical R744 supermarket refrigeration systems based on advanced exergy analysis. *Energy Convers. Manag.* **2021**, *229*, 113684. [CrossRef]
24. Erbay, Z.; Hepbasli, A. Application of conventional and advanced exergy analyses to evaluate the performance of a ground-source heat pump (GSHP) dryer used in food drying. *Energy Convers. Manag.* **2014**, *78*, 499–507. [CrossRef]
25. Kline, S.J.; McClintock, F.A. Describing uncertainties in single sample experiments. *Mech. Eng.* **1953**, *75*, 3–8.
26. Lemmon, E.W.; Bell, I.H.; Huber, M.L.; McLinden, M.O. *NIST Standard Reference Database 23: Reference Fluid Thermodynamic and Transport Properties-REFPROP*; version 10.0; Standard Reference Data Program; National Institute of Standards and Technology: Gaithersburg, MD, USA, 2018.